

RESEARCH PAPER

Characterization of two cotton cDNAs encoding *trans*-2-enoyl-CoA reductase reveals a putative novel NADPH-binding motif

Wen-Qiang Song^{1,2}, Yong-Mei Qin^{1,2,*}, Mihoko Saito³, Tsuyoshi Shirai³, François M. Pujol⁴, Alexander J. Kastaniotis⁴, J. Kalervo Hiltunen⁴ and Yu-Xian Zhu^{1,2}

¹ National Laboratory of Protein Engineering and Plant Genetic Engineering, College of Life Sciences, Peking University, Beijing, 100871, China

² Department of Biochemistry and Molecular Biology, College of Life Sciences, Peking University, Beijing, 100871, China

³ Department of Bioscience, Nagahama Institute of Bioscience and Technology, 1266 Tamura, Nagahama 526-0829, Japan

⁴ Biocenter Oulu and Department of Biochemistry, University of Oulu, PO Box 3000, FI-90014 Oulu, Finland

Received 10 November 2008; Revised 5 February 2009; Accepted 13 February 2009

Abstract

Very long chain fatty acids are important components of plant lipids, suberins, and cuticular waxes. *Trans*-2-enoyl-CoA reductase (ECR) catalyses the fourth reaction of fatty acid elongation, which is NADPH dependent. In the present study, the expression of two cotton *ECR* (*GhECR*) genes revealed by quantitative RT-PCR analysis was up-regulated during cotton fibre elongation. *GhECR1* and *2* each contain open reading frames of 933 bp in length, both encoding proteins consisting of 310 amino acid residues. GhECRs show 32% identity to *Saccharomyces cerevisiae* Tsc13p at the deduced amino acid level, and the *GhECR* genes were able to restore the viability of the *S. cerevisiae* haploid *tsc13*-deletion strain. A putative non-classical NADPH-binding site in GhECR was predicted by an empirical approach. Site-directed mutagenesis in combination with gas chromatography–mass spectrometry analysis suggests that G(5X)IPXG presents a putative novel NADPH-binding motif of the plant ECR family. The data suggest that both *GhECR* genes encode functional enzymes harbouring non-classical NADPH-binding sites at their C-termini, and are involved in fatty acid elongation during cotton fibre development.

Key words: 2-Enoyl-CoA reductase, fatty acid elongation, *Gossypium hirsutum*, NADPH-binding motif, very long chain fatty acid.

Introduction

In higher plant cells, *de novo* fatty acid synthesis occurs in plastids, whereas fatty acid elongation, as in mammalian cells, occurs in the endoplasmic reticulum (ER) (Cinti *et al.*, 1992; Ohlrogge and Browse, 1995; Poulos, 1995). Plant very long chain fatty acids (VLCFAs, fatty acids >C18), either saturated or monounsaturated, are important precursors of sphingolipids, seed triacylglycerols, suberins, and cuticular waxes (Kunst and Samuels, 2003; Chen *et al.*, 2006, 2008). Plant free fatty acids or their derivatives may also serve directly as signalling molecules (Kachroo *et al.*, 2003; Qin *et al.*, 2007a). Fatty acid elongation uses malonyl-CoA as the

two-carbon donor and proceeds via four successive reactions: a condensation of malonyl-CoA with a long chain acyl substrate producing a 3-ketoacyl-CoA catalysed by 3-ketoacyl-CoA synthase (KCS); a reduction of 3-ketoacyl-CoA to 3-hydroxyacyl-CoA catalysed by 3-ketoacyl-CoA reductase (KCR); a dehydration of 3-hydroxyacyl-CoA to *trans*-2-enoyl-CoA catalysed by 3-hydroxyacyl-CoA dehydratase (HCD); and a second reduction of *trans*-2-enoyl-CoA to acyl-CoA catalysed by *trans*-2-enoyl-CoA reductase (ECR) (Cinti *et al.*, 1992; Poulos, 1995). Following the successful identification of a yeast HCD gene, *PHS1* (Denic

* To whom correspondence should be addressed. E-mail: qinym@pku.edu.cn
© 2009 The Author(s).

and Weissman, 2007), a complete set of *Arabidopsis* genes encoding the enzymes catalysing each distinct step is now available (Lassner *et al.*, 1996; Todd *et al.*, 1999; Beaudoin *et al.*, 2002; Han *et al.*, 2002; Zheng *et al.*, 2005; Bach *et al.*, 2008; Joubès *et al.*, 2008).

The first gene encoding a microsomal ECR was initially identified as *TSC13* in the yeast *Saccharomyces cerevisiae* by a genetic screening method (Beeler *et al.*, 1998). Disruption of *ScTSC13* (*tsc13Δ*) resulted in an accumulation of ceramides that harbour fatty acids shorter than 26 carbons (Kohlwein *et al.*, 2001). ScTsc13p has a six membrane-spanning topology (Paul *et al.*, 2007), and is targeted to nuclear–vacuolar junctions (Kvam *et al.*, 2005). Orthologues of ScTsc13p were subsequently identified in mouse, humans, and *Arabidopsis thaliana* (Moon and Horton, 2003; Gable *et al.*, 2004). Disruption of the *Arabidopsis ECR* gene affects shoot growth and morphogenesis (Zheng *et al.*, 2005). In cotton, *KCS* and *KCR* genes were functionally characterized and VLCFAs were found to promote fibre cell elongation by activating ethylene synthesis (Qin *et al.*, 2005, 2007a, b). The plant ECRs share no sequence similarities with 2-enoyl thioester reductases involved in other eukaryotic fatty acid-metabolizing processes, including cytosolic, peroxisomal, and mitochondrial, as well as prokaryotic fatty acid synthesis pathways (Smith, 1994; Airenne *et al.*, 2003; Gloerich *et al.*, 2006; Zhang *et al.*, 2006). The reduced form of nicotinamide adenine dinucleotide phosphate (NADPH) operates chiefly with enzymes that synthesize energy-rich molecules. All the ECR enzymes characterized this far catalyse an NADPH-dependent reaction that reduces the double bond of *trans*-2-enoyl thioester to acylthioester. Although NAD(P)H was shown to be utilized in the two reductive steps of fatty acid synthesis and elongation (Harlan and Wakil, 1963; Beaudoin *et al.*, 2002; Qin *et al.*, 2005), the amino acid sequences of GhECRs lacked either the canonical Rossmann fold signature GXGXXG/A (Rao and Rossmann, 1973) or other well-characterized NADP/NAD-binding motifs in the PROSITE database, such as the glyceraldehyde 3-phosphate dehydrogenase active site or D-isomer-specific 2-hydroxyacid dehydrogenases NAD-binding signatures (Sigrist *et al.*, 2002).

In this study, two putative cotton *GhECR* genes were identified in developing cotton fibre cells. Complementation of the growth-deficient yeast *tsc13Δ* mutant by the cotton gene was performed to examine the *in vivo* function of *GhECR*. A further investigation into the complex structures of nucleotide-binding protein in the Protein Data Bank (Berman *et al.*, 2003) revealed a weak similarity of the region 225-GSGGYQIPH/RG-234 of GhECRs to several nucleotide-binding motifs. The newly proposed NAD(P)H-binding motif was tested by point mutational analyses.

Materials and methods

Plant materials

Upland cotton (*Gossypium hirsutum* L. cv. Xuzhou 142) and fuzzless-lintless mutant (*fl*) cotton ovules were planted in

a fully automated greenhouse. Since the *fl* mutant has no fibre cells growing on the ovules, it is often used as a control for identification of genes expressed preferentially in fibre (Ji *et al.*, 2003). Fresh cotton ovules at various day(s) post-anthesis (dpa), leaves, flowers, stems, and roots were harvested immediately at the indicated times and frozen in liquid nitrogen before performing the RNA preparation.

RNA extraction and quantitative real-time PCR (qRT-PCR)

The cotton fibres were stripped from ovules growing at 3, 5, 10, 15, and 20 dpa. Total RNA was extracted from wild-type cotton ovules, fibres, flowers, leaves, stems, roots, and *fl* ovules (Ji *et al.*, 2003; Shi *et al.*, 2006). Leaves of 10 d to 16 d old which developed on the apical dome were used as young leaves. Cotton cDNA was reverse-transcribed from 5 µg of total RNA with the gene-specific primers: *GhECR1*, 5'-TGGGAGCGGAGGCTATCAA-3' (forward, F) and 5'-GTCCATCGAGTAGGAAGTTTTACCC-3' (reverse, R); *GhECR2*, 5'-GGTTCGGGTTTGGTATAGTTTG-3' (F) and 5'-AAGTACGATGCTCATCGATCC-3' (R). qRT-PCR was performed with the SYBR green PCR kit (Applied Biosystems) in a DNA Engine Opticon-Continuous Fluorescence Detection System (MJ Research) in triplicate using independent RNA samples. The cotton ubiquitin gene *UBQ7* was used as internal control in each reaction.

For detection of the transcripts of *GhECR2* or *ScTSC13* in the yeast cells, RT-PCR was performed using the following primers: *GhECR2*, 5'-TTGAGCTTAATGACTCGGCTACTG-3' (F) and 5'-CGCTTTTCTTCGTATCCAAAGTAC-3' (R); *ScTSC13*, 5'-CACAATATCAGCAAGTACAGGA-3' (F) and 5'-CCGAATGAAATGAGACCG-3' (R).

Yeast strains and media

The *S. cerevisiae* diploid strain W1536 *TSC13/tsc13Δ* (MAT *a*α; *ade2Δ/ade2Δ*; *ade3Δ/ade3Δ*; *can1-100/can1-100*; *his3-11,15/his3-11,15*; *leu2-3, 112/leu2-3, 112*; *trp1-1/trp1-1*; *ura3-1/ura3-1*; *tsc13Δ::kanMX4/TSC13*) was made by transformation of a PCR-amplified *tsc13Δ::kanMX4* fragment from genomic DNA of *S. cerevisiae* BY4743 *TSC13/tsc13Δ* (MAT *a*α; *his3Δ1/his3Δ1*; *leu2Δ0/leu2Δ0*; *met15Δ0/met15Δ0*; *ura3Δ0/ura3Δ0*; *tsc13Δ::kanMX4/TSC13*, EURO-SCARF) containing the *TSC13*-flanking region. Yeast media were prepared and cells were grown according to standard procedures (Sherman *et al.*, 1986).

Construction of plasmids

The open reading frames of *GhECR1* and 2 were amplified using the primers listed in Table S1 available at JXB online, restricted with *Bam*HI–*Eco*RI and *Bam*HI–*Xho*I, respectively, purified with the Qiagen PCR purification kit, and ligated into the *TRP1*-marked pYADE4 behind the *ADHI* promoter, resulting in the generation of plasmids pYADE4-*GhECR1* and pYADE4-*GhECR2*. The plasmid pYADE4-*GhECR2* served as a template in PCRs for constructing all

of the mutant variants with *GhECR2*-specific primers (Supplementary Table S1), using a QuikChange site-directed mutagenesis kit (Stratagene). The nucleotide sequences of wild-type *GhECR* genes and all mutants of *GhECR2* were confirmed by DNA sequencing. As a control, cDNA of *ScTSC13* was amplified and cloned into *URA3*-marked *YCplac33* behind the *GALI* promoter.

Heterologous expression of cotton GhECRs in yeast cells

The plasmid pYADE4-*GhECR* was transformed into the W1536 *TSC13/tsc13A* yeast strain. The transformants were selected on synthetic complete medium lacking tryptophan (Sc-Trp) plates and sporulated. The growing ascospores were digested with zymolase (Seikagaku) and the tetrads were dissected using a Singer MSM manual dissection microscope (Singer Instruments). The mutant spores complemented by *GhECR* were replica plated on a YPD-G418 (YPD supplemented with 300 µg of geneticin ml⁻¹) plate and a 2-amino-5-fluorobenzoic acid (FAA) plate [synthetic complete medium containing 2% (w/v) D-glucose and 0.05% (w/v) FAA] simultaneously. Spores carrying the *tsc13A::kanMX4* knock-out allele and complemented by the pYADE4-*GhECR* plasmid were identified by their resistance to G418 (geneticin), and their inability to grow on FAA plates. To verify that the *GhECR* gene was essential for the survival of the *tsc13A* mutant, the mutant cells carrying pYADE4-*GhECR* were transformed by pYES2-*GhECR* that was constructed using the primers listed in Supplementary Table S1 at JXB online. The plasmid, pYES2-*GhECR*, had a *URA3* marker fused with a gene fragment encoding a His-tag behind the C-terminus of GhECR. Cell viability on the FAA plate was restored.

Preparation of ER extracts from yeast cells

Yeast cells transformed by the pYADE4-*GhECR* plasmid were grown to exponential phase in Sc-Trp medium at 30 °C. The cells were harvested, disrupted with glass beads, and centrifuged for 15 min at 15 000 g, at 4 °C. The total lysate was centrifuged for 90 min at 85 000 g in a Sorval Ti70 rotor at 4 °C, generating the supernatant (S85) and the pellet (P85), which is an ER fraction. The protein concentration was determined by the Lowry method using bovine serum albumin as the standard.

Fatty acid extractions and gas chromatography–mass spectrometry (GC-MS) analysis

Wild-type haploid *S. cerevisiae* W1536B cells or *tsc13A* mutant cells were transformed by pYADE4-*GhECR* and its variants. Yeast cells were homogenized by bead beating; subsequently fatty acids were extracted and converted to methyl esters (FAMES) according to the method described by Cahoon and Lynch (1991). The resultant FAMES were separated on a DB-225MS column from the Agilent 6890N GC system coupled to an HP5973 mass detector. The National Institute of Standards and Technology and Wiley

databases were applied for compound identification. C17 fatty acid (heptadecanoic acid, Sigma-Aldrich) was added as an internal standard before extraction for monitoring sample recovery and quantification.

Immunoblotting

Immunoblotting was performed as described previously (Qin *et al.*, 2005), using ECL™ western blotting detection reagents (Amersham Biosciences). Recombinant GhECR was detected by using mouse monoclonal antibody against His-tag as the primary antibody (Invitrogen) and affinity-purified goat anti-mouse IgG conjugated to horseradish peroxidase as the secondary antibody. The *S. cerevisiae* ER marker protein Kar2p (a gift from Dr M Rose) was used as the primary antibody, and goat anti-rabbit IgG conjugated to horseradish peroxidase as the secondary antibody.

Binding motif search

A non-redundant set of nucleotide-binding protein structures was prepared from the Protein Data Bank. All of the structures binding NADP/NAD or similar nucleotides were extracted from the database, and the proteins showing >25% sequence identity were clustered (Saito *et al.*, 2006). The final set contained 62 non-redundant proteins. The GhECR sequences were compared with these sequences to detect similarities with the nucleotide-binding sites. Conservation of the detected motifs was confirmed by using the Conserved Domain Database (CDD) at NCBI (Marchler-Bauer *et al.*, 2007). Also, the motifs were compared with the PROSITE database to detect a possible similarity to the characterized motifs (Sigrist *et al.*, 2002).

Results

The GhECR2 gene is highly expressed during cotton fibre development

Relative transcript levels of *GhECRs* from 3, 5, 10, 15, and 20 dpa wild-type cotton fibres were quantified by qRT-PCR analysis. The transcript level of *GhECR1* increased close to 3-fold and that of *GhECR2* increased ~9-fold in 10 dpa fibres compared with their levels in 0 dpa ovules (Fig. 1A). *GhECR2* was predominantly expressed in the fibres and young leaves compared with the ovules, whereas expression was low in roots, stems, mature leaves, and flowers, and *fl* mutant ovules (Fig. 1B), indicating that *GhECR2*, but not *GhECR1*, was associated with fibre development.

Cloning and prediction of the NADPH-binding site for GhECRs

Nucleotide sequence analyses indicated that both *GhECR1* and *GhECR2* possess 933 bp open reading frames encoding polypeptides of 310 amino acids with 89% sequence identity. GhECR1 and 2 share 81–83% sequence identity with AtECR, 82–83% with NbECR, 36–37% with human or rat ECRs, and 27–28% with *S. cerevisiae* Tsc13p.

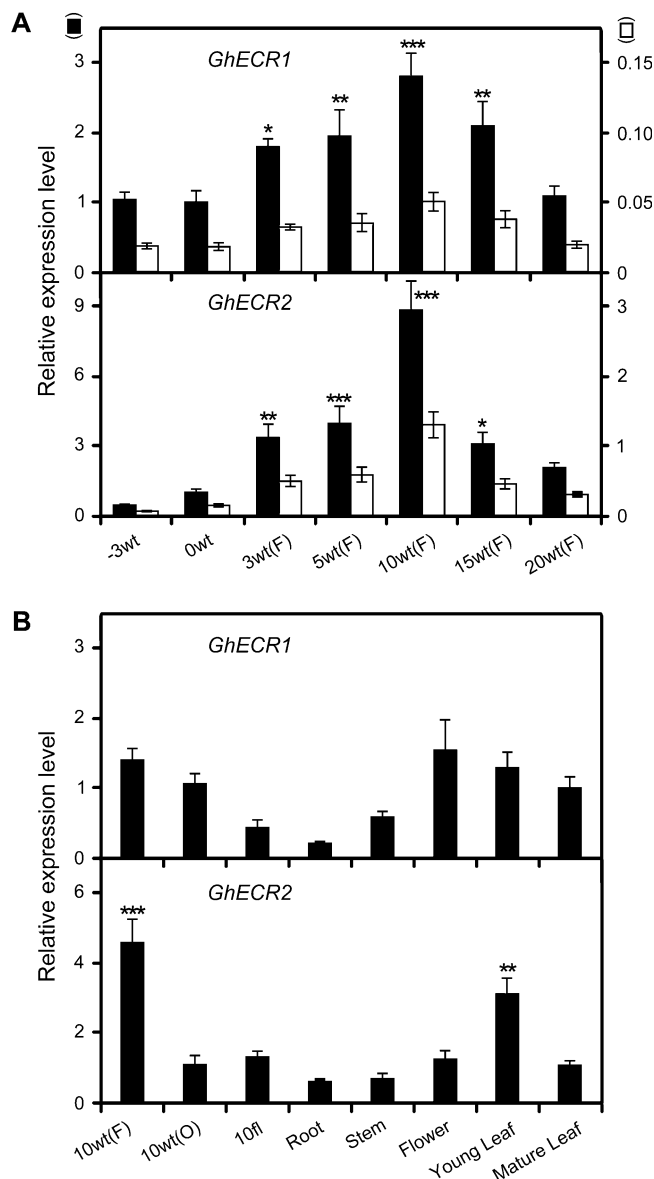


Fig. 1. Quantitative real-time PCR analyses of transcript levels of *GhECR* genes in wild-type cotton ovules, fibres, variable cotton tissues, and mutant cotton ovules. -3, 0, 3, 5, 10, 15, and 20 dpa, and 10fl indicate that total RNA samples prepared from wild-type or fl mutant cotton ovules (O) or fibres (F) were used as template for qRT-PCR analysis. Solid bars with scales to their left indicate the fold increase relative to the values of 0 dpa (A) or 10 dpa wild-type ovules (B) (arbitrarily set to 1) of the same *GhECR* gene. Open bars with scales to their right indicate the fold increase of each *GhECR* relative to cotton *UBQ7* (GenBank accession no. AY189972). Statistical significance was determined using one-way ANOVA software combined with Tukey's test throughout this figure. * $P < 0.05$; ** $P < 0.01$; *** $P < 0.001$.

In order to predict NADP/NAD-binding sites in GhECRs, the sequences were compared with known nucleotide-binding motifs in the structure database (Saito *et al.*, 2006). As a result, no protein showed strong similarity with GhECRs in their binding sites. However, a few motifs, including that of the nudix hydrolase-15

domain, showed weak similarities to the glycine-rich region 225-GSGGYQIPH/RG-234 of GhECRs. Because most known motifs for nucleotide binding are glycine rich (Rao and Rossmann, 1973), this was identified as the primary candidate for the NADP/NAD-binding site of GhECRs. This anticipation was supported by sequence alignment of residues L220–F235 of GhECRs with the C-termini of rat and human 5α -steroid reductases (Fig. 2B), which catalyse reductions of the double bond between the 4 and 5 carbon atoms of steroids. G184 (G188) was shown to be involved in the NADP/NAD binding of the rat (human) enzyme (Russell and Wilson, 1994; Bhattacharyya and Collins, 2001).

Functional characterization of wild-type cotton *ECR* genes in the yeast *tsc13Δ* mutant

Tsc13p, as the only protein with ECR function in VLCFA production in *S. cerevisiae*, is essential for survival in cells (Kohlwein *et al.*, 2001). To address the biological function of the cotton genes, the viability of the *tsc13Δ* mutant cells complemented by *GhECR* was examined. As shown in Supplementary Fig. S1 at *JXB* online and in Fig. 3A, the lethality of the *tsc13Δ* mutant was rescued when the mutant cells were transformed by yeast expression plasmids carrying the cotton genes. In agreement with the plate assay, *tsc13Δ* mutant cells expressing *GhECR1* and 2 as C-terminally His-tagged proteins showed growth rates close to that of wild-type yeast cells (Fig. 3B). The ER fractions (P85) were separated from the supernatant fractions (S85) by differential centrifugation using total proteins extracted from yeast cells. Immunoblotting of each of the fractions using anti-6×His and anti-ScKar2p indicated that GhECR1 or 2 were present in the same fraction where the ER marker ScKar2p was found (Fig. 3C). Production of VLCFA, especially C26:0, was detected in the *tsc13Δ* mutant cells expressing *GhECR* genes (Fig. 3D; Supplementary Table S2). Taken together, the data presented here indicated that both of the *GhECR* genes were able to complement the synthetic lethal phenotype of *tsc13Δ* and hence were expressing functional cotton ECRs.

Identification of amino acid residues involved in the NADPH-binding site of *GhECR2*

As shown in Fig. 2B, the region G225–G234 from both GhECRs was predicted to be involved in binding of NADPH. A complete set of point mutations was constructed in which single amino acid residues of GhECR2 in this region were changed into alanine by site-directed mutagenesis, and the resulting cotton ECR mutants were expressed in the *tsc13Δ* mutant. Of the mutant proteins tested, six restored the growth defect of the *tsc13Δ* cells on Sc+FAA plates, as did the wild-type GhECR2 (Fig. 4A). However, the four mutants G225A, I231A, P232A, and G234A were not able to complement the *tsc13Δ* mutant (Fig. 4A). Immunoblot analysis confirmed that all these variants were present at similar levels to wild-type GhECR2

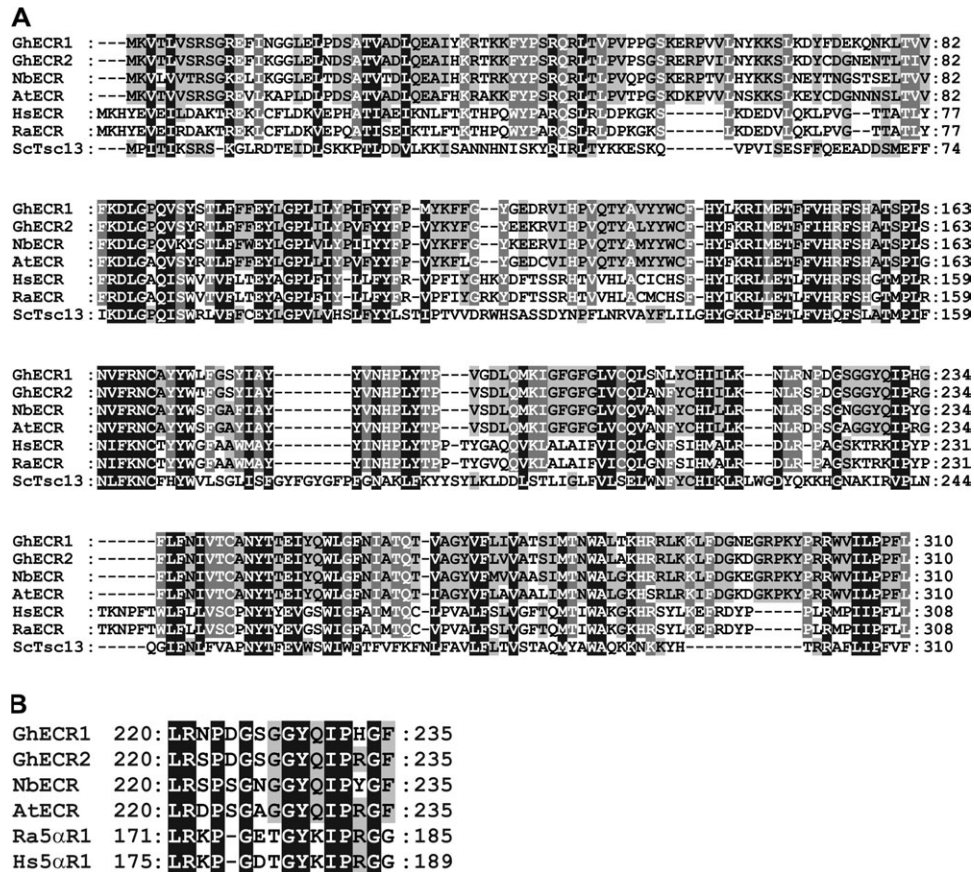


Fig. 2. Amino acid sequence alignment of GhECR1 and GhECR2. (A) Amino acid sequence alignment of GhECR1 (GenBank accession no. ABV60088) and GhECR2 (ABV60089) with orthologues from *A. thaliana* (NP_191096), *N. benthamiana* (AAY17262), humans (AAP36986), rat (NP_612558), and *S. cerevisiae* (NP_010269). Black shading indicates strictly conserved residues, whereas grey shading indicates regions with less strict conservation. (B) Amino acid sequence alignment of plant ECRs with rat and human 5 α -steroid reductases identified a putative NADPH-binding region.

(Fig. 4B). These data revealed that G225, I231, P232, and G234 were critical for the functions of GhECR2.

Mutated GhECR causes a significantly low level of VLCFA

To investigate the effects of the mutated GhECR, the yeast *tscl3A* mutant transformed by both YCplac33-*ScTSC13* and pYADE4-*GhECR2* was used. A high concentration of glucose is able to shut off the expression of *ScTSC13*, which is under the control of the *GAL1* promoter. When the yeast cells were inoculated from the culture medium containing 2% galactose to medium containing 4% glucose, the growth rates of *tscl3A* cells expressing mutated *GhECR* genes became slow after 10 h (Fig. 5A). RT-PCR analyses showed that the transcript levels of *ScTSC13* decreased in culture medium containing 4% glucose compared with those in 2% galactose (Fig. 5B). Transcription of *GhECR2* and its variants was not affected by 4% glucose (Fig. 5C), which was further verified by immunoblotting analyses (Fig. 5D). To avoid non-specific effects caused by prolonged growth inhibition, glucose-treated yeast cells were studied at 12 h after glucose supplementation. Quantitative analyses of the

fatty acid composition of yeast cells transformed with wild-type *GhECR2* by GC-MS revealed a major product of C26:0 in the cells, whereas the levels of C26:0 and C24:0 were significantly decreased in the four GhECR2 mutated variants (Fig. 5E; Supplementary Fig. S2 at *JXB* online). Instead, significant accumulation of fatty acids C22:0, C20:0, C18:0, C18-OH, and especially C16-OH was detected in the *tscl3A* cells expressing the GhECR mutated proteins (Fig. 5E). These data suggest that the four residues, G225, I231, P232, and G234, participate in GhECR2 catalysis of VLCFA biosynthesis.

A new candidate for the NADPH-binding motif for GhECR

The topology of GhECR2 was predicted based on that of AtECR (Paul *et al.*, 2007). Based on the analyses of the different mutants, the location of the NADPH-binding motif of GhECR2 was proposed to be facing the cytosolic side of the ER membrane (Fig. 6A). The sequence G(5X)IPXG is comparable with the NADP/NAD-binding sites of NMN adenylyltransferase/ADP ribose pyrophosphatase (PDB code 2qjo), UDP-glucose dehydrogenase

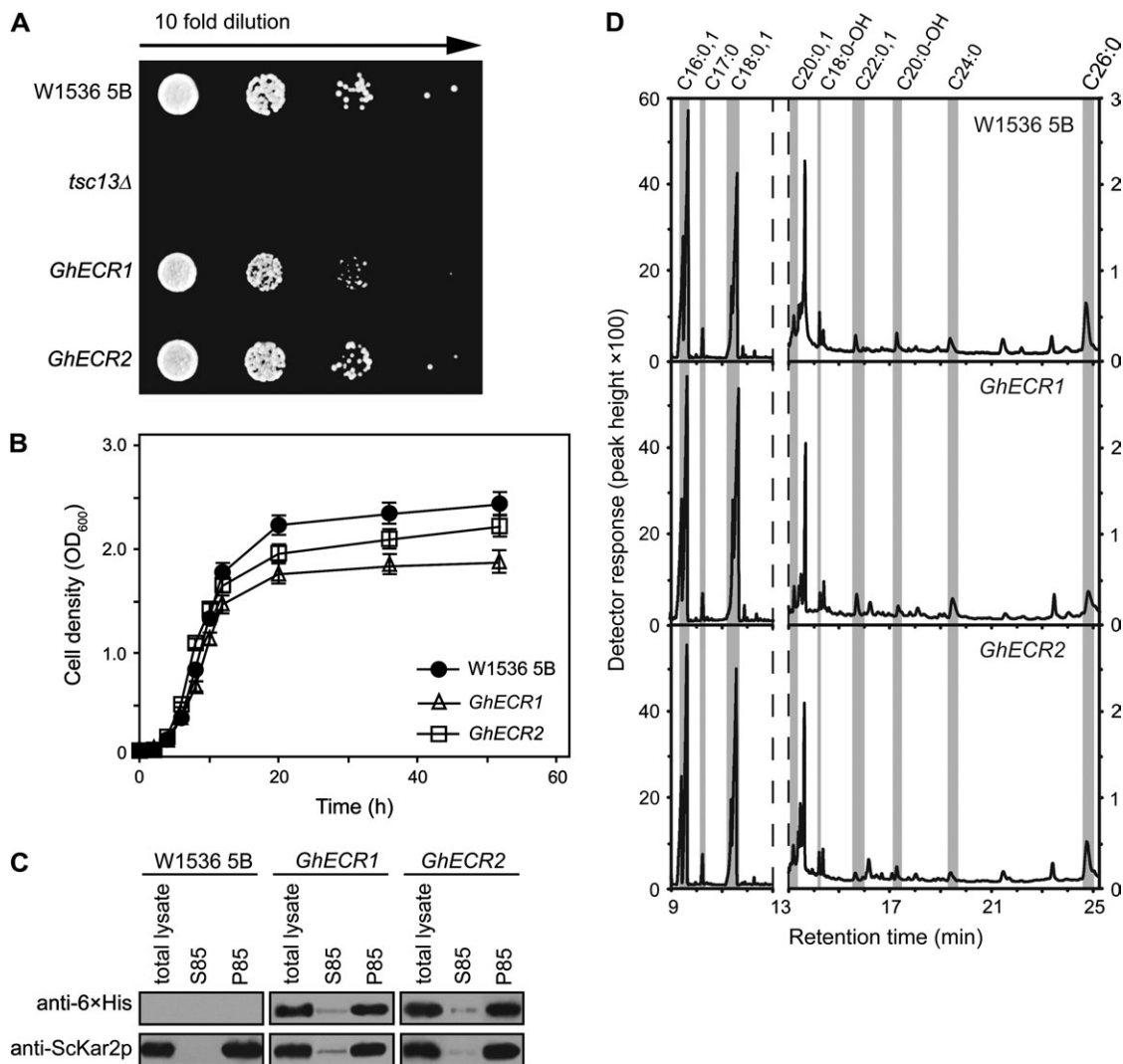


Fig. 3. The viability of *S. cerevisiae tsc13Δ* mutant cells is restored by functional complementation of individual *GhECR* genes. (A) Complementation of *S. cerevisiae tsc13Δ* mutant cells by individual *GhECR* genes. (B) Growth curve of *S. cerevisiae tsc13Δ* mutant cells expressing *GhECR1* or 2. (C) *GhECR*s were localized in microsomal fractions together with the ER marker *ScKar2p*. The fractions of the supernatant (S85) and the pellet (P85) were separated from the total lysate (see Materials and methods). (D) GC analyses of total fatty acids extracted from wild-type W1536 5B and *tsc13Δ* mutant cells complemented by *GhECR1* or 2.

(PDB code 1d1j), and the general stress protein GSP69 (PDB code 1pz1) (Fig. 6B). These amino acids, except for G225, were highly conserved in the nudix hydrolase-15 domain for which the three-dimensional structures are known (NMN adenylyltransferase/ADP ribose pyrophosphatase, Fig. 6B, C). According to the structure, the counterparts of I231, P232, and G234 (L230, P231, and G233 in Fig. 6C, respectively) existed close to the nucleotide ligand, giving further credence to the suggestion that they may be involved in the binding of NADPH.

Discussion

VLCFA biosynthesis plays important roles during plant development (Zheng *et al.*, 2005; Chen *et al.*, 2006; Qin *et al.*, 2007a) and its regulation was reported to be mediated

by a MYB transcription factor in *Arabidopsis* (Raffaele *et al.*, 2008). *ECR* catalyses the last step of VLCFA biosynthesis and is proposed to be a ubiquitous component of elongase complexes of different plant tissues (Park *et al.*, 2005; Zheng *et al.*, 2005). In this study, two cotton *ECR* genes were cloned, overexpressed, and characterized. Judging from the expression profiles of *GhECR* genes, *GhECR2* may be involved in the cotton fibre fast elongating stage (Fig. 1). This is consistent with the fact that the transcripts of other genes encoding enzymes of VLCFA synthesis as well as production of VLCFAs in cotton fibre cells significantly increased at the same time (Qin *et al.*, 2005, 2007a, b; Shi *et al.*, 2006). Elevated biosynthesis of VLCFAs during the fibre cell rapid elongation period implicated VLCFAs to serve as precursors of signalling molecules, sphingolipids, and cuticular wax in the process (Zheng *et al.*, 2005; Qin *et al.*, 2007a). In other plants, the absence

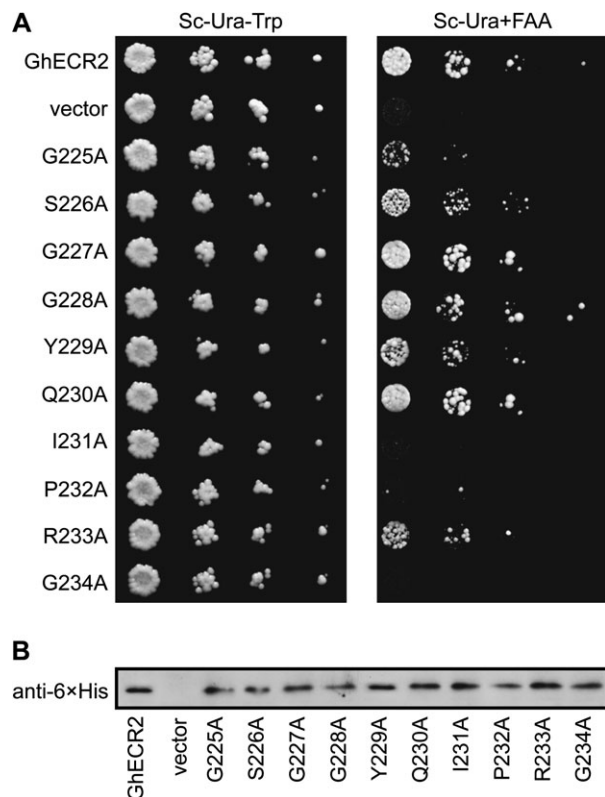


Fig. 4. Screening of GhECR2 variants involved in the putative NADPH-binding site. (A) GhECR2 variants were generated by site-directed mutagenesis and were tested for their activity by complementation of the *S. cerevisiae tsc13Δ* mutant. Sc-Ura-Trp, synthetic complete medium containing 2% (w/v) D-glucose, but lacking uracil and tryptophan; Sc-Ura+FAA, synthetic complete medium containing 2% (w/v) D-galactose, 0.05% (w/v) D-glucose, and 0.05% (w/v) FAA, but lacking uracil. (B) GhECR2 variants were detected by immunoblotting with anti-6xHis antibody.

or suppression of ECR activity resulted in a reduction of VLCFAs (Park *et al.*, 2005; Zheng *et al.*, 2005), emphasizing the function of ECR in fatty acid elongation. Consistent with the fact that higher plants produce variable VLCFA-containing lipids, suberin, and waxes, *GhECR2* was also shown to be important for the development of leaves (Fig. 1B).

The reaction catalysed by ECR reduces the (*trans*-2) double bond of *trans*-2-enoyl-CoA, similar to the activity of characterized 2-enoyl thioester reductases of fatty acid synthesis (Smith, 1994; Airene *et al.*, 2003; Gloerich *et al.*, 2006; Zhang *et al.*, 2006). Both cotton ECRs were demonstrated to be functional homologues of ScTsc13p by their ability to rescue the growth of the *tsc13Δ* mutant (Fig. 3). Comparison of the GhECR2 amino acid sequence with the sequences of the other NADPH-binding proteins leads to the identification of a candidate NADPH-binding site (Fig. 2B). In order to determine the importance of this sequence for the protein function, a number of cotton GhECR2 mutants were engineered by site-directed mutagenesis and tested for complementation of the yeast *tsc13Δ*

mutant (Fig. 4). Four residues, G225, I231, P232, and G234, of GhECR2 were shown to be essential for GhECR2 activity (Fig. 4), since substitution of any of the residues by alanine resulted in a loss of growth of *tsc13Δ* cells, and the decrease of GhECR activity in yeast cells caused a significant reduction of VLCFA biosynthesis (Fig. 5E and Supplementary Fig. S2 at *JXB* online). Accumulation of C18:0, C20:0, and C22:0, but not C24:0, caused by the variable mutated GhECR2 proteins suggests that GhECR2 has chain length specificity towards the *trans*-2-enoyl-CoAs which have >24 carbons. This may explain the reason why cotton requires a second *ECR* gene encoding the enzyme that is responsible for elongation of fatty acids longer than C22. Interestingly, accumulation of hydroxylated long chain fatty acids with C16 chain length was another consequence (Fig. 5E and Supplementary Fig. S2), similar to the higher C16-OH content detected in the *Arabidopsis ECR* mutant *cer10* (Zheng *et al.*, 2005), suggesting that plant ECR affected the biosynthesis of complex sphingolipids in eukaryotes. It is noteworthy that the counterpart of GhECR2 G225 in NMN adenylyltransferase/ADP ribose pyrophosphatase is not directly involved in binding of NADPH (G224 in Fig. 6C). This residue is also not conserved among the nudix hydrolase-15 domains, while it is highly conserved among GhECR homologues (Fig. 2A). Though it appears that none of the known motifs could fully explain each of the important residues of GhECR detected in this study, the G(5X)IPXG motif of the GhECR family can be considered to represent a putative novel NADPH-binding motif, or at least a new variation of the nudix hydrolase-15 motif with a significant change in conformation.

The membrane topology of GhECR2 prediction based on the topology of AtECR (Paul *et al.*, 2007) revealed that the protein spans the membrane six times and that their N- and C-termini are facing the cytosol (Fig. 6A). The proposed NADPH-binding motif G(5X)IPXG is located in a loop between transmembrane domains 4 and 5 (Fig. 6A). This motif positioning at the cytosolic face of the ER membrane was not the site where the catalytic residues were indicated previously (Paul *et al.*, 2007). The oxidative pentose phosphate pathway is a major source of NADPH for biosynthetic processes such as fatty acid synthesis in non-photosynthetic cells (Debnam and Emes, 1999; Neuhaus and Emes, 2000). Hence, the location of the identified motif was implied to be favoured for binding of the cytosolic NADPH. In conclusion, this study constituted the first characterization of cotton ECRs during cotton fibre elongation, and established a non-classical NADPH-binding motif which was essential for activity. The use of yeast microsomal membranes as a source of protein limits the extent of our studies. The possibilities that the four identified residues affecting GhECR2 activity might be independent of NADPH binding cannot be excluded. Therefore, efforts are underway to engineer GhECRs for structure–function studies, including a direct observation of the molecular interactions between the putative NADPH-binding motif and the cofactor, with purified enzymes in the future.

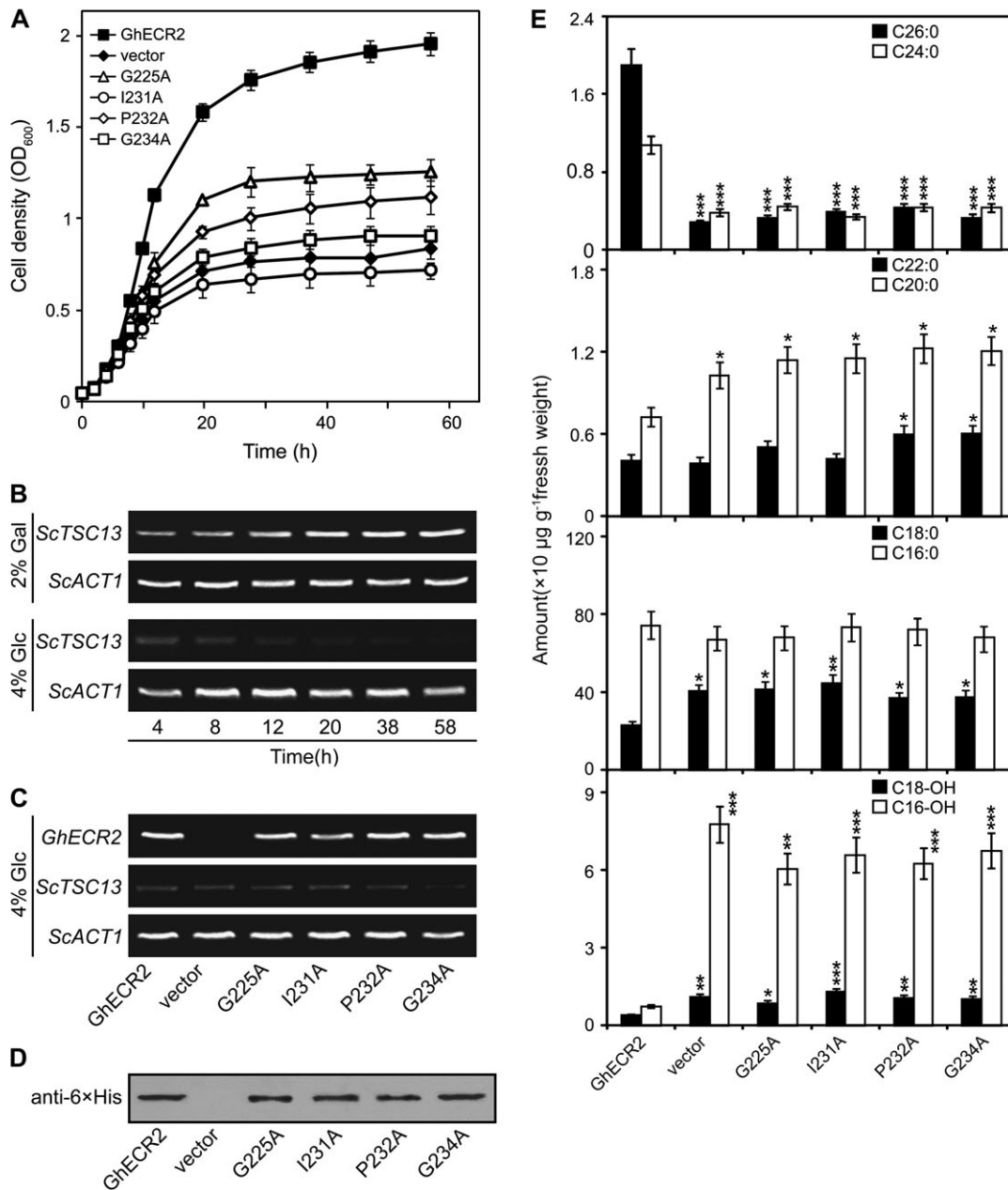


Fig. 5. Mutated GhECR2 caused reduction of VLCFAs and accumulation of hydroxylated long chain fatty acids. (A) The *tsc13Δ* mutant cells expressing *ScTSC13* and the *GhECR2* variant were pre-inoculated in synthetic medium containing 2% galactose. Following dilution of an overnight culture to a fresh synthetic medium containing 4% glucose, starting from OD_{600 nm} equal to 0.05, the cell density as a determination of growth was measured. (B) RT-PCR analyses of transcript levels of *ScTSC13* in medium containing 4% glucose at the indicated time, compared with those obtained in 2% galactose. (C) RT-PCR analyses of expression of *GhECR2* and its variants in medium containing 4% glucose at 12 h. (D) The important mutated GhECR2 proteins were detected to be expressed by immunoblotting. (E) GC analyses of total fatty acids extracted from the *tsc13Δ* mutant cells expressing important *GhECR2* variants when the transcription of *ScTSC13* was inhibited by 4% glucose at 12 h. Statistical significance was determined using one-way ANOVA software combined with Tukey's test throughout this figure. **P* < 0.05; ***P* < 0.01; ****P* < 0.001.

Supplementary data

Supplementary data are available at *JXB* online.

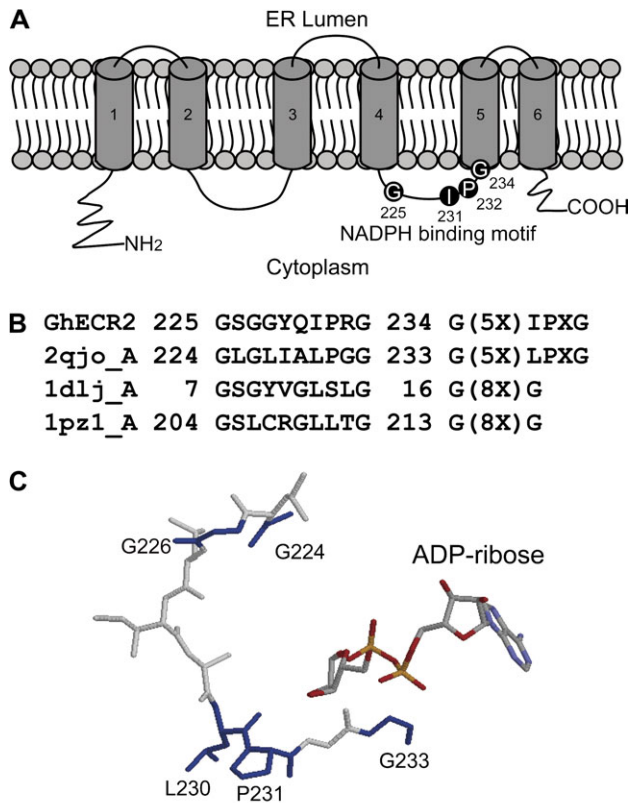
Fig. S1. The tetrad dissection of diploid W1536 *TSC13/tsc13Δ* cells transformed with pYADE4-*GhECR*.

Fig. S2. GC spectra of long chain fatty acids (LCFAs) and very long chain fatty acids (VLCFAs) from the *tsc13Δ*

mutant complemented by wild-type *GhECR2* and its mutant variants.

Table S1. The primers used in the current study.

Table S2. Quantitative analysis of the fatty acid composition of wild-type yeast and *tsc13Δ* mutant cells complemented by *GhECR1* or *GhECR2* as reported in Fig. 3.



2qjo: NMN Adenylyl transferase/ADP-ribose pyrophosphatase

Fig. 6. G(5X)IPXG is a putative novel NADPH-binding motif of GhECR. (A) The position of G(5X)IPXG in the six-membrane-spanning topology of GhECR2. (B) The similarity of putative NADPH-binding sites of GhECR2 to NMN adenylyltransferase/ADP ribose pyrophosphatase (PDB code 2qjo), UDP-glucose dehydrogenase (PDB code 1d1j), and general stress protein GSP69 (PDB code 1pz1). (C) The structure of the nucleotide-binding motif of NMN adenylyltransferase/ADP ribose pyrophosphatase with bound ADP-ribose. Sites identical to GhECR are shown in blue.

Acknowledgements

This work was supported by grants from National Basic Research Program of China (Grant no. 2004CB117302), the National High-tech Research Program of China (Grant nos 2006AA10A109-1 and 2007AA10Z136), the Sigrid Jusélius Foundation of Finland, and the Academy of Finland. We thank Professor Wolf-Hubert Kunau of Ruhr University for the pYADE4 vector.

References

- Airenne TT, Torkko JM, Van den plas S, Sormunen RT, Kastaniotis AJ, Wierenga RK, Hiltunen JK. 2003. Structure–function analysis of enoyl thioester reductase involved in mitochondrial maintenance. *Journal of Molecular Biology* **327**, 47–59.
- Beaudoin F, Gable K, Sayanova O, Dunn T, Napier JA. 2002. A *Saccharomyces cerevisiae* gene required for heterologous fatty acid elongase activity encodes a microsomal β -keto-reductase. *Journal of Biological Chemistry* **277**, 11481–11488.
- Bach L, Michaelson LV, Haslam R, et al. 2008. The very-long-chain hydroxy fatty acyl-CoA dehydratase PASTICCINO2 is essential and limiting for plant development. *Proceedings of the National Academy of Sciences, USA* **105**, 14727–14731.
- Beeler T, Bacikova D, Gable K, Hopkins L, Johnson C, Slife H, Dunn T. 1998. The *Saccharomyces cerevisiae* TSC10/YBR265w gene encoding 3-ketosphinganine reductase is identified in a screen for temperature-sensitive suppressors of the Ca^{2+} -sensitive *csg2Δ* mutant. *Journal of Biological Chemistry* **273**, 30688–30694.
- Berman HM, Henrick K, Nakamura H. 2003. Announcing the worldwide Protein Data Bank. *Nature Structural Biology* **10**, 980.
- Bhattacharyya AK, Collins DC. 2001. Site-directed mutagenesis studies of rat steroid 5 α -reductase (isozyme-1): mutation of residues in the cofactor binding and C-terminal regions. *Journal of Steroid Biochemistry and Molecular Biology* **77**, 177–182.
- Cahoon EB, Lynch DV. 1991. Analysis of glucocerebrosides of rye (*Secale cereale* L. cv Puma) leaf and plasma membrane. *Plant Physiology* **95**, 58–68.
- Chen M, Han G, Dietrich CR, Dunn TM, Cahoon EB. 2006. The essential nature of sphingolipids in plants as revealed by the functional identification and characterization of the *Arabidopsis* LCB1 subunit of serine palmitoyltransferase. *The Plant Cell* **18**, 3576–3593.
- Chen M, Markham JE, Dietrich CR, Jaworski JG, Cahoon EB. 2008. Sphingolipid long-chain base hydroxylation is important for growth and regulation of sphingolipid content and composition in *Arabidopsis*. *The Plant Cell* **20**, 1862–1878.
- Cinti DL, Cook L, Nagi MN, Suneja SK. 1992. The fatty acid chain elongation system of mammalian endoplasmic reticulum. *Progress in Lipid Research* **31**, 1–51.
- Debnam PM, Emes MJ. 1999. Subcellular distribution of enzymes of the oxidative pentose phosphate pathway in root and leaf tissues. *Journal of Experimental Botany* **50**, 1653–1661.
- Denic V, Weissman JS. 2007. A molecular caliper mechanism for determining very long-chain fatty acid length. *Cell* **130**, 663–677.
- Gable K, Garton S, Napier JA, Dunn TM. 2004. Functional characterization of the *Arabidopsis thaliana* orthologue of Tsc13p, the enoyl reductase of the yeast microsomal fatty acid elongating system. *Journal of Experimental Botany* **55**, 543–545.
- Gloerich J, Ruitter JP, van den Brink DM, Ofman R, Ferdinandusse S, Wanders RJ. 2006. Peroxisomal *trans*-2-enoyl-CoA reductase is involved in phytol degradation. *FEBS Letters* **580**, 2092–2096.
- Harlan WR Jr, Wakil SJ. 1963. Synthesis of fatty acids in animal tissues. I. Incorporation of C14-acetyl coenzyme A into a variety of long chain fatty acids by subcellular particles. *Journal of Biological Chemistry* **238**, 3216–3223.
- Han G, Gable K, Kohlwein SD, Beaudoin F, Napier JA, Dunn TM. 2002. The *Saccharomyces cerevisiae* YBR159w gene encodes the 3-ketoreductase of the microsomal fatty acid elongase. *Journal of Biological Chemistry* **277**, 35440–35449.
- Ji SJ, Lu YC, Feng JX, Wei G, Li J, Shi YH, Fu Q, Liu D, Luo JC, Zhu YX. 2003. Isolation and analyses of genes preferentially expressed during early cotton fiber development by subtractive PCR and cDNA array. *Nucleic Acids Research* **31**, 2534–2543.

- Joubès J, Raffaele S, Bourdenx B, Garcia C, Laroche-Traineau J, Moreau P, Domergue F, Lessire R.** 2008. The VLCFA elongase gene family in *Arabidopsis thaliana*: phylogenetic analysis, 3D modelling and expression profiling. *Plant Molecular Biology* **67**, 547–566.
- Kachroo A, Lapchyk L, Fukushige H, Hildebrand D, Klessig D, Kachroo P.** 2003. Plastidial fatty acid signaling modulates salicylic acid- and jasmonic acid-mediated defense pathways in the *Arabidopsis ssi2* mutant. *The Plant Cell* **15**, 2952–2965.
- Kohlwein SD, Eder S, Oh CS, Martin CE, Gable K, Bacikova D, Dunn T.** 2001. Tsc13p is required for fatty acid elongation and localizes to a novel structure at the nuclear–vacuolar interface in *Saccharomyces cerevisiae*. *Molecular and Cellular Biology* **21**, 109–125.
- Kunst L, Samuels AL.** 2003. Biosynthesis and secretion of plant cuticular wax. *Progress in Lipid Research* **42**, 51–80.
- Kvam E, Gable K, Dunn TM, Goldfarb DS.** 2005. Targeting of Tsc13p to nucleus–vacuole junctions: a role for very-long-chain fatty acids in the biogenesis of microautophagic vesicles. *Molecular Biology of the Cell* **18**, 3987–3998.
- Lassner MW, Lardizabal K, Metz JG.** 1996. A jojoba β -ketoacyl-CoA synthase cDNA complements the canola fatty acid elongation mutation in transgenic plants. *The Plant Cell* **8**, 281–292.
- Marchler-Bauer A, Anderson JB, Derbyshire MK, et al.** 2007. CDD: a conserved domain database for interactive domain family analysis. *Nucleic Acids Research* **35**, D237–D240.
- Moon Y-A, Horton JD.** 2003. Identification of two mammalian reductases involved in the two-carbon fatty acyl elongation cascade. *Journal of Biological Chemistry* **278**, 7335–7343.
- Neuhaus HE, Emes MJ.** 2000. Nonphotosynthetic metabolism in plastids. *Annual Review of Plant Physiology and Plant Molecular Biology* **51**, 111–140.
- Ohlrogge J, Browse J.** 1995. Lipid biosynthesis. *The Plant Cell* **7**, 957–970.
- Park JA, Kim TW, Kim SK, Kim WT, Pai HS.** 2005. Silencing of *NbECR* encoding a putative enoyl-CoA reductase results in disorganized membrane structures and epidermal cell ablation in *Nicotiana benthamiana*. *FEBS Letters* **579**, 4459–4464.
- Paul S, Gable K, Dunn TM.** 2007. A six-membrane-spanning topology for yeast and *Arabidopsis* Tsc13p, the enoyl reductases of the microsomal fatty acid elongating system. *Journal of Biological Chemistry* **282**, 19237–19246.
- Poulos A.** 1995. Very long chain fatty acids in higher animals. *Lipids* **30**, 1–14.
- Qin YM, Pujol FMA, Shi YH, Feng JX, Liu YM, Kastaniotis AJ, Hiltunen JK, Zhu YX.** 2005. Cloning and functional characterization of two cDNAs encoding NADPH-dependent 3-ketoacyl-CoA reductase from developing cotton fibers. *Cell Research* **15**, 465–473.
- Qin YM, Hu CY, Pang Y, Kastaniotis AJ, Hiltunen JK, Zhu YX.** 2007a. Saturated very-long-chain fatty acids promote cotton fiber and *Arabidopsis* cell elongation by activating ethylene biosynthesis. *The Plant Cell* **19**, 3692–3704.
- Qin YM, Pujol FM, Hu CY, Feng JX, Kastaniotis AJ, Hiltunen JK, Zhu YX.** 2007b. Genetic and biochemical studies in yeast reveal that the cotton fibre-specific GhCER6 gene functions in fatty acid elongation. *Journal of Experimental Botany* **58**, 473–481.
- Raffaele S, Vaillau F, Léger A, Joubès J, Miersch O, Huard C, Blée E, Mongrand S, Domergue F, Roby D.** 2008. A MYB transcription factor regulates very-long-chain fatty acid biosynthesis for activation of the hypersensitive cell death response in *Arabidopsis*. *The Plant Cell* **20**, 752–767.
- Rao S, Rossmann M.** 1973. Comparison of super-secondary structures in proteins. *Journal of Molecular Biology* **76**, 241–256.
- Russell DW, Wilson JD.** 1994. Steroid 5 α -reductase: two genes/two enzymes. *Annual Review of Biochemistry* **63**, 25–61.
- Saito M, Go M, Shirai T.** 2006. An empirical approach for detecting nucleotide-binding sites on proteins. *Protein Engineering Design and Selection* **19**, 67–75.
- Sherman F, Fink GR, Hicks JB.** 1986. *Methods in yeast genetics*. Cold Spring Harbor, NY: Cold Spring Harbor Laboratory Press.
- Shi YH, Zhu SW, Mao XZ, Feng JX, Qin YM, Zhang L, Cheng J, Wei LP, Wang ZY, Zhu YX.** 2006. Transcriptome profiling, molecular biological, and physiological studies reveal a major role for ethylene in cotton fiber cell elongation. *The Plant Cell* **18**, 651–664.
- Sigrist CJA, Cerutti L, Hulo N, Gattiker A, Falquet L, Pagni M, Bairoch A, Bucher P.** 2002. PROSITE: a documented database using patterns and profiles as motif descriptors. *Briefings in Bioinformatics* **3**, 265–274.
- Smith S.** 1994. The animal fatty acid synthase: one gene, one polypeptide, seven enzymes. *FASEB Journal* **8**, 1248–1259.
- Todd J, Post-Beittenmiller D, Jaworski JG.** 1999. KCS1 encodes a fatty acid elongase 3-ketoacyl-CoA synthase affecting wax biosynthesis in *Arabidopsis thaliana*. *The Plant Journal* **17**, 119–130.
- Zhang YM, White SW, Rock CO.** 2006. Inhibiting bacterial fatty acid synthesis. *Journal of Biological Chemistry* **281**, 17541–17544.
- Zheng H, Rowland O, Kunst L.** 2005. Disruptions of the *Arabidopsis* enoyl-CoA reductase gene reveal an essential role for very-long-chain fatty acid synthesis in cell expansion during plant morphogenesis. *The Plant Cell* **17**, 1467–1481.